

Article

Not peer-reviewed version

Tidal Flat Extraction and Analysis in China Based on Multi-source Remote Sensing Image Collection and MSIC-OA Algorithm

[JiXiang_Sun](#) , [Cheng_Tang](#) ^{*} , Ke Mu , [Yanfang_Li](#) , [Xiangyang_Zheng](#) , [Tao_Zou](#)

Posted Date: 16 July 2024

doi: 10.20944/preprints2024071304.v1

Keywords: remote sensing; Google Earth Engine; MSIC-OA; tidal flat resources; shoreline



Preprints.org is a free multidiscipline platform providing preprint service that is dedicated to making early versions of research outputs permanently available and citable. Preprints posted at Preprints.org appear in Web of Science, Crossref, Google Scholar, Scilit, Europe PMC.

Copyright: This is an open access article distributed under the Creative Commons Attribution License which permits unrestricted use, distribution, and reproduction in any medium, provided the original work is properly cited.

Article

Tidal Flat Extraction and Analysis in China Based on Multi-Source Remote Sensing Image Collection and MSIC-OA Algorithm

Jixiang Sun ^{1,2,3}, Cheng Tang ^{1,2,*}, Ke Mu ^{1,2,3}, Yanfang Li ^{1,2}, Xiangyang Zheng ^{1,2} and Tao Zou ^{1,2}

¹ CAS Key Laboratory of Coastal Environmental Processes and Ecological Remediation, Yantai Institute of Coastal Zone Research, Chinese Academy of Sciences, Yantai 264003, China;

² Shandong Provincial Key Laboratory of Coastal Zone Environmental Processes, Yantai 264003, China;

³ University of Chinese Academy of Sciences, Beijing 100049, China

* Correspondence: ctang@yic.ac.cn

Abstract: As an important part of coastal wetlands, tidal flats provide unique ecosystem services and functions. China's tidal flats are significantly threatened by industrialization, urbanization, aquaculture expansion and coastline reconstruction, and there is an urgent need for sustainable strategies to balance the protection and utilization of tidal flats. Remote sensing technology can realize large-scale spatiotemporal research of tidal flats, comprehensively improve the ecological environment of coastal zones, and help achieve the overall planning goals of major projects for the protection and restoration of important ecosystems in China. In this study, based on GEE (Google Earth Engine) platform, Sentinel-2 (MSI), Landsat 8 (OLI) and Landsat 9 (OLI-2) remote sensing images were used to construct multi-source intensive time series remote sensing image collection, combined with MSIC-OA algorithm. The tidal flat data of China in 2018 and 2023 are extracted and analyzed. The results show as follows: 1) The overall classification accuracy of the tidal flat in 2023 is 95.19%, and the Kappa coefficient is 0.89; In 2018, they were 92.77% and 0.83 respectively. 2) The total tidal flat area in 2018 and 2023 is 8300.34km² and 8151.54km², respectively, a decrease of 148.80km²; 3) In 2023, estuarine and bay tidal flats will account for 54.88% of the total area, and most of the tidal flats will be distributed near river inlets and bays; 4) In 2023, the total length of the coastline adjacent to the tidal flat is 10196.17km, of which the artificial shoreline accounts for 67.06%, and the development degree of the tidal flat is 2.04, indicating that most of the tidal flat has been developed and utilized. The research results provide valuable reference for the scientific planning and rational utilization of tidal flat resources in China.

Keywords: remote sensing; Google Earth Engine; MSIC-OA; tidal flat resources; shoreline

1. Introduction

Tidal flats, including intertidal mudflats, rocks, and sandy beaches, are transitional zones between Marine and terrestrial environments ^[1,2]. The tidal flat in this study is defined as the silty or sandy unvegetated coast in the tide-flooded area between the maximum and minimum tidal inundation, including the part of the radiating sand ridge, which is geomorphologically called the "intertidal zone" ^[3].

Tidal flats provide unique ecosystem services, such as defending against storm surges, maintaining shorelines, filtering pollutants and promoting carbon storage, as well as serving as feeding grounds for migratory birds and spawning and feeding grounds for fish and other Marine wildlife ^[4-6]. As one of the world's most important ecological and economic ecosystems, tidal flats are very fragile and highly threatened by tidal reclamation and natural disturbance ^[7,8]. Under the influence of rapid socio-economic development and climate change in the coastal zone, the depletion of coastal wetland resources is very serious ^[9]. According to the latest report, about 35% of the world's coastal wetlands were lost from 1970 to 2015 ^[10]. Sustainable management of coastal tidal flats has been included in the Sustainable Development Goals of the 2030 Agenda of the United Nations ^[11]. Studies have shown that in the context of climate change, maintaining the longterm stability of the

tidal flat wetland ecosystem is of great significance to achieving the joint Sustainable Development Goals in coastal areas^[12, 13].

Over the past four decades, China's coastal tidal flats have been under development. Industrialization, urbanization and the expansion of aquaculture have been significantly threatened^[14-16]. More than two-thirds of China's coastline has been converted into artificial sea walls, causing a series of damage to tidal flats^[17]. The government has made great efforts to restore and manage degraded coastal ecosystems in order to achieve the Sustainable Development Goals related to sustainable management of coastal resources^[18]. In 2020, China issued the Master Plan for Major National Projects for the Protection and Restoration of Important Ecosystems (2021-2035), which takes the restoration of shoreline and shoal as the main direction for the comprehensive improvement of coastal ecological environment in the future^[19]. Since China began to gradually pay attention to the protection of coastal wetlands in 2003, there is still much room for improvement in the protection and restoration of coastal wetlands in China^[20-22]. Tidal flat reclamation brings huge local economic benefits^[23].

In recent years, the evolution of tidal flats has been increasingly affected by human activities, resulting in rapid degradation of tidal flats^[24, 25]. Artificial structures built on the tidal flats cut off the exchange of terrestrial and Marine materials, inhibit the natural process of sediment migration and deposition, and accelerate the erosion and shrinkage of the tidal flats^[26,27]. Artificial development activities alter the depth and velocity of the sea-land exchange capacity, thus altering the sedimentation process of the tidal flat^[28]. Artificial reclamation shortens the natural sedimentary path, allowing more fine particulate matter to enter the Marine system directly, causing tidal flat erosion^[29]. Long-term observation studies in the reclamation area of the tidal flat in Jiangsu show that continuous reclamation has destroyed the original balance of erosion and deposition of the tidal flat, resulting in the degradation and shrinkage of the tidal flat^[30]. Therefore, it is necessary to expound the utilization status and development trend of tidal flat comprehensively. This paper provides a basis for the protection and restoration of tidal flats^[31, 32].

Google Earth Engine (GEE) is a cloud computing platform developed by Google for satellite data analysis and processing, which has been widely used in large-scale remote sensing research. GEE cloud platform includes all Landsat, Sentinel-1, Sentinel-2 and other satellite data; And other data sets such as weather data, land cover data, and even socioeconomic data.

At present, the lack of macroscopic and accurate surface spatial survey data and the lack of periodic tidal flat resource information in China greatly limit the spatio-temporal analysis of the dynamic changes of tidal flats in China. Aiming at the limitations of existing tidal flat maps, this research plan selects Sentinel-2, Landsat8 and Landsat9 images as data sources based on GEE platform, and constructs multi-source intensive time-series remote sensing image collection. The refined mapping of China's tidal flats in 2018 and 2023 was carried out with the improved MSIC-OA algorithm to provide scientific data support and theoretical basis for the development and management of coastal zone resources.

2. Materials and Methods

2.1. Study Area

Stretching from the mouth of the Yalu River in the north to the mouth of the Beilun River in the south, China's coastal belt spans more than 20 latitudes (18. 2 degrees to 40. 5 degrees north) with a coastline of about 18, 000 kilometers. It covers a total of 12 provincial-level administrative units in Liaoning, Tianjin, Hebei, Shandong, Jiangsu, Shanghai, Zhejiang, Fujian, Guangdong (including Hong Kong and Macao special administrative Regions), Guangxi Zhuang Autonomous Region, Hainan and Taiwan Province (Figure 1). From north to south, the coastal areas, with average annual temperatures ranging from 5 ° C to 26 ° C and precipitation ranging from 400 to 1,800 mm, cover the three climate zones of hot zone, subtropical zone and temperate climate. The elevations of China's coastal zone range from sea level to more than 3,700 meters above sea level, with most of the northern half being low-lying, although some mountains and hills in northeast China and the Shandong

Peninsula extend all the way to the coastal areas. The main landscapes of China's intertidal zone include tidal flats, mangroves, salt marshes, aquaculture ponds, building land, and waters.

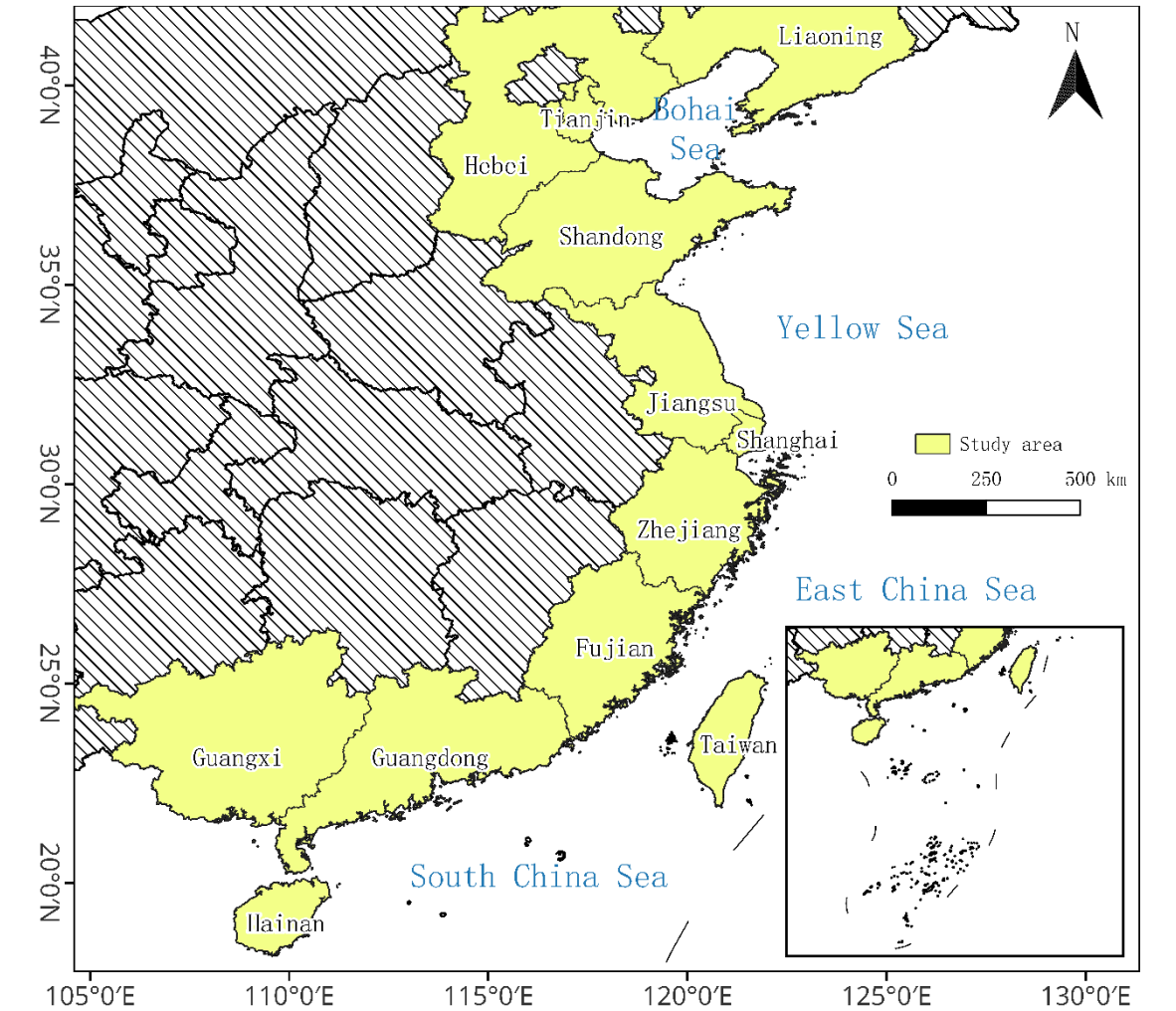


Figure 1. Study area.

2.2. Data Sources

Sentinel-2 data used in this study are surface reflectance products after atmospheric correction processing at level 2A (L2A), and Landsat 8/9 data are Collection 2 Tier 1 atmospheric top reflectance data products. The time range is 2017.07-2019.06 and 2022.07-2024.06. The image band parameters are shown in Table 1. The QA60 band of Sentinel-2 image and QA_PIXEL band of Landsat image are used for cloud removal. For Sentinel-2 images, SWIR 1 band is sampled up to 10 m spatial resolution by bilinear interpolation. For Landsat 8 and Landsat 9 images, atmospheric correction was performed first, and then panchromatic bands with a spatial resolution of 15 m were used. GS image fusion method was adopted to sample the multispectral bands to a spatial resolution of 15 m. After up-sampling processing, the spatial resolution of Sentinel-2 and Landsat multi-spectral bands selected were 10m and 15m, respectively. The above operations are implemented on the GEE platform.

Table 1. Satellite image data parameters.

Satellite	Band	resolution/m
Sentinel-2 (MSI)	B3 (Green)	10
	B4 (Red)	10
	B8 (NIR)	10
	B11 (SWIR1)	20

Landsat 8 (OLI)	B3 (Green)	30
	B4 (Red)	30
	B5 (NIR)	30
	B6 (SWIR1)	30
	B8 (Panchromatic)	15
Landsat 9 (OLI-2)	B3 (Green)	30
	B4 (Red)	30
	B5 (NIR)	30
	B6 (SWIR1)	30
	B8 (Panchromatic)	15

2.3. Extraction of Tidal Flat

The process of automatic, rapid and high-precision tidal flat extraction constructed in this study is shown in Figure 2.

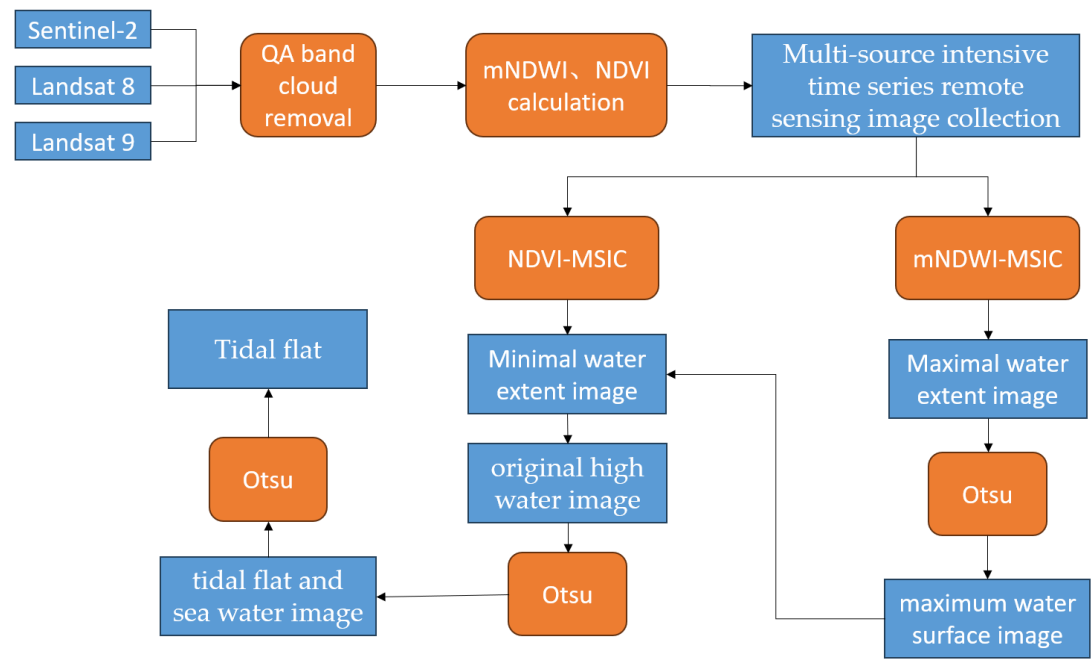


Figure 2. Technical route.

The MSIC algorithm first selects the quality band, and then sorts the quality band pixel by pixel. The maximum value after sorting is taken as the final output value of the pixel. Otsu (OA) algorithm, based on gray histogram, finds the best threshold and divides the image into background and foreground, which makes the inter-class variance maximum and intra-class variance minimum.

According to the research results of (Jia et al., 2021) [33], the improved normalized differential water body index mNDWI and normalized differential vegetation index NDVI were used in this study to extract the maximum and minimum water areas respectively. The mNDWI formula is:

$$mNDWI = \frac{Green - Swir1}{Green + Swir1} \tag{1}$$

where, *Green* is the green light band of the image, *Swir1* is the short-wave infrared band 1 of the image.

The NDVI formula is:

$$NDVI = \frac{Nir - Red}{Nir + Red} \tag{2}$$

where, *Nir* is the near infrared band of the image, and *Red* is the red band of the image.



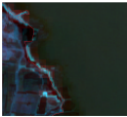
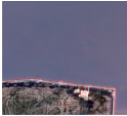

Some results of tidal flat extraction include tidal flat and floating mud. To solve this problem, OA binary segmentation of tidal flat floating mud image is needed to achieve the purpose of accurate extraction of tidal flat.

2.4 extraction and classification of shoreline

2.4. Extraction and Classification of Shoreline

According to the technical regulations for coastal repair of China's Offshore Marine Comprehensive Survey and Evaluation Project (908 Project), China's coastline is divided into natural shoreline (land and sea boundary line under natural land and sea action) and artificial shoreline (actual land and sea boundary line formed after artificial reconstruction) according to the actual type of shoreline of China's coast and the research objective of this study. Canny edge detection method is used to extract the upper boundary of the tidal flat as the shoreline, and the shoreline is classified by artificial visual interpretation (Table 2).

Table 2. Coastline classification system.

Primary Classification	Secondary Classification	Interpretation Symbol	Description
Natural Shoreline	Sandy Shoreline		Located in sandy beach areas
	Mud Shoreline		Located in mud or silt-sand mudflat areas
	Rocky Shoreline		Located in rocky coastal areas
Artificial Shoreline	Engineered Embankment		Located in urban and transportation construction areas, including shorelines formed by port and dock construction
	Non-engineered Embankment		Regularly distributed patches such as aquaculture water bodies, farmland, and salt fields on the inland side

The Tidal Flat Development Degree Index (TFDDI) is established to directly reflect the development degree of tidal flats, as follows:

$$TFDDI = \frac{L_1}{L_2}$$

(3)

In the formula, TFDDI refers to the development degree of a tidal flat in a certain area, and L1 and L2 respectively refer to the length of artificial shoreline and natural shoreline in the coastline adjacent to the tidal flat in this area. The larger the TFDDI value, the higher the development degree of the tidal flat.

3. Results

3.1. precision Analysis of Tidal Flat Extraction

In order to check the accuracy of the experimental extraction results, the quantitative and qualitative analysis of the tidal flat extraction results were carried out in this study. The quantitative analysis combined the lowest tide Sentinel-2 and Landsat images and randomly generated sample points to verify the accuracy of the extraction results. The information of tidal flats and non-tidal flats was distinguished by artificial visual interpretation, and the accuracy of the range of tidal flats in all observation periods was evaluated by combining the confusion matrix method. The confusion matrices of tidal flats in 2018 and 2023 were obtained respectively (Table 3): The overall accuracy and kappa coefficient of the tidal flat extraction results in 2018 reached 92.77% and 0.83, respectively. In 2023, it will reach 95.19% and 0.89 respectively.

Table 3. Confusion matrix and precision analysis.

		Reference Category			Use. Acc/%	Pro.Acc/%	Ove. Acc/%	Kappa
		TF	Non- TF	Total				
2018	TF	2772	308	3080	90.00	96.98	92.77	0.83
	Non- TF	415	6505	6920	94.00	95.48		
	Image Category	Total	3187	6813	10000			
2023	TF	2752	272	3024	91.01	92.94	95.19	0.89
	Non- TF	209	6767	6976	97.00	96.14		
	Total	2961	7039	10000				

Qualitative analysis combined with UQD data (2017-2019) produced by Murray et al on GEE platform, selected three typical regions of Liao River Estuary, Caofeidian and central Jiangsu, and compared the extracted tidal flats in 2018 with UQD data. It was found that the UQD was basically consistent with the extracted tidal flats in this study. However, Murray et al. extracted the tidal flat in the 50km buffer zone of the coastline and mistakenly extracted the inland surface objects as the tidal flat, resulting in a large difference between the extraction results on the land side and those in this study (Figures 3, 4, 5). In summary, the results of tidal flat extraction in this study are reliable. In summary, the accuracy of the tidal flat extraction results in this study is reliable.

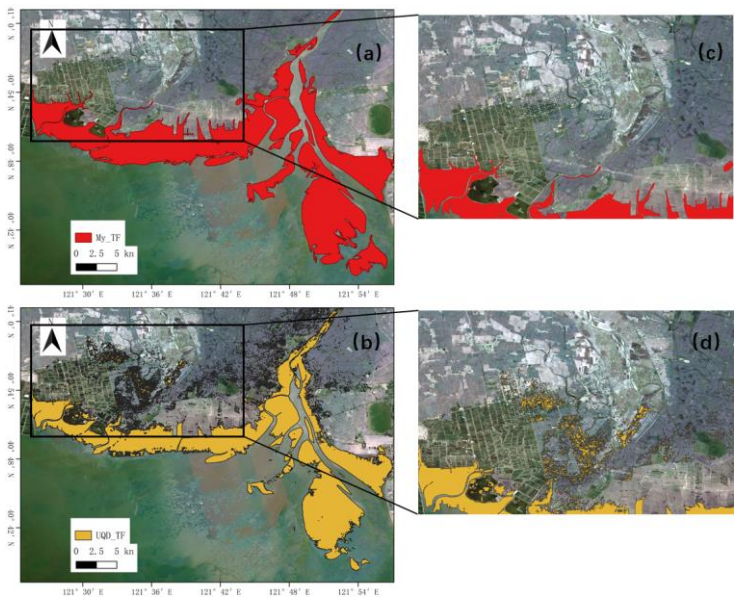


Figure 3. The comparison of the accuracy of the extraction results of the tidal flat in Liao River Estuary with the UQD map.

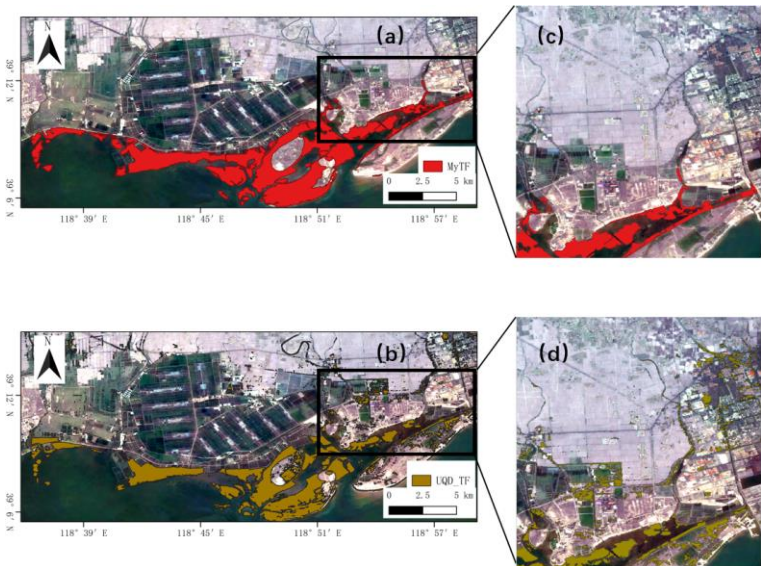


Figure 4. The comparison of the accuracy of the extraction results of the tidal flat in Caofeidian with the UQD map.

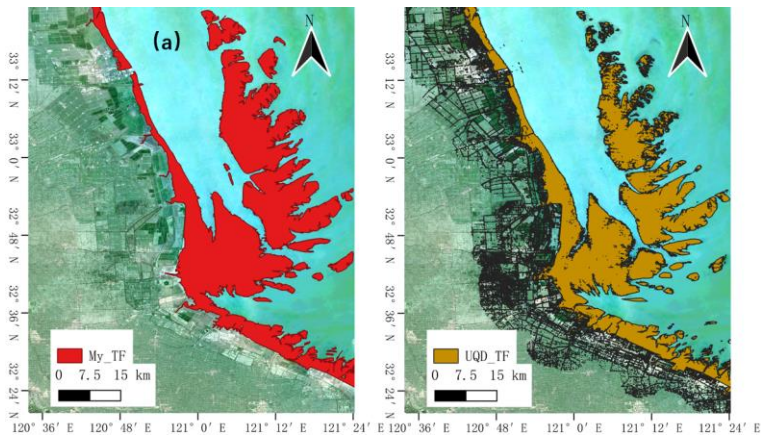


Figure 5. The comparison of the accuracy of the extraction results of the tidal flat in the radiating shoal tidal flat area in central Jiangsu with the UQD map.

3.2. *tidal Flat Stock*

The total area of tidal flat stock in China in 2023 is 8151.54km² (Table 4). The largest tidal flat area is in Jiangsu Province (2149.01 km²), accounting for 26.36%. The smallest city is Tianjin (55.33 km²), accounting for 0.68%.

Table 4. Area and Proportion of Tidal Flats in China in 2023.

Region	Area (km ²)	Proportion (%)
Liaoning	923.44	11.33
Hebei	222.63	2.73
Tianjin	55.33	0.68
Shandong	1150.07	14.11
Jiangsu	2149.01	26.36
Shanghai	384.94	4.72
Zhejiang	1189.49	14.59
Fujian	1006.13	12.34
Guangdong	425.45	5.22
Guangxi	329.63	4.04
Hainan	77.90	0.96
Taiwan	237.52	2.91
China	8151.54	100.00

In the estuarine area, sediment deposition becomes very significant due to abundant sediment sources and sufficient supply; In addition, the wave energy divergence effect in the bay is significant, the disturbance effect of wind waves is small, and the large tidal changes lead to the formation of a large amount of sediment accumulation here. From the perspective of spatial distribution of tidal flats, tidal flats are divided into estuarine, bay and others three categories, and the specific information after classification is shown in Figure 6. The tidal flat area of estuarine and bay was 1828.08 km² and 2644.82km², accounting for 22.43% and 32.45% respectively, accounting for 54. 88% in total. In other provinces and cities except Jiangsu Province, the total tidal flat area is 6002.53 km², and the total tidal flat area of estuarine and bay is 1785.14km² and 2574. 83 km², accounting for 29.74% and 42.90% respectively, accounting for 72.64% in total(Figure 6). It can be seen that most of the tidal flats in China are distributed near the estuaries and bays of rivers.

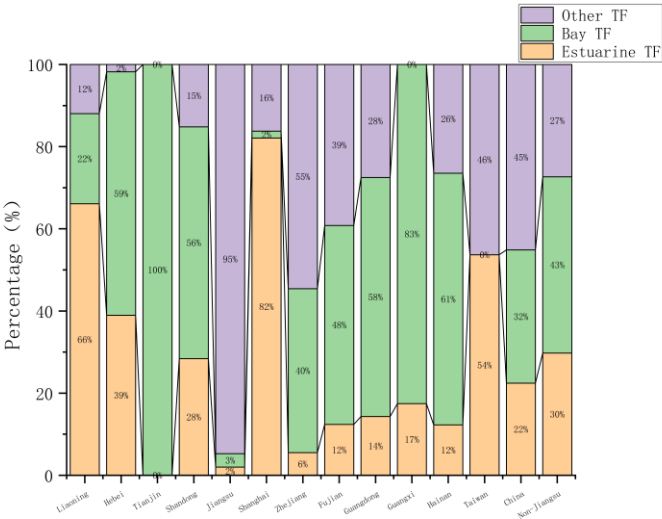


Figure 6. Stacked Percentage Chart of Tidal Flat Classification.

3.3. Spatial Distribution of Tidal Flats

The spatial distribution of tidal flats in China in 2023 is shown in Figure 7. The tidal flats of Liaoning Province will mainly be distributed in the coastline of the Yellow Sea and the Liao River estuary of Liaodong Bay in the east of the province, accounting for 43.98% and 39.73%, respectively. The tidal flats in Hebei Province will be mainly distributed along the Daqing Estuary and Bohai Bay, accounting for 36.81% and 59.22%, respectively. All tidal flats in Tianjin will be located in Bohai Bay, mainly on both sides of Tianjin Port, accounting for 56.98% in the north and 43.02% in the south. The tidal flats in Shandong Province will mainly be distributed in Bohai Bay, Laizhou Bay and Yellow River delta, accounting for 15.49%, 31.09% and 25.74%, respectively. The main distribution area of the tidal flat in Jiangsu Province will be from Sheyang Estuary to the estuary of the Yangtze River, accounting for 91.63%.The main distribution area of the tidal flat in Shanghai will be the estuary of the Yangtze River, accounting for 82.12%.The distribution of tidal flats in Zhejiang Province is relatively fragmented, and the tidal flats in Hangzhou Bay area are relatively large, accounting for 28.57%. The tidal flats of Fujian Province are evenly distributed along the long and winding coastline. The tidal flats in Guangdong Province are very fragmented, located in Zhanjiang in the southwest of Guangdong Province. The tidal flat area of Zhanjiang City is relatively large, accounting for 51.50%. Among them, the tidal flat area of Beibu Gulf in the west is 116.24 km², accounting for 27.32%; The tidal flat area of Leizhou Bay and its vicinity in the east is 102.86km², accounting for 24.18%. All the tidal flats in Guangxi Province will be located in Beibu Gulf and distributed evenly. The tidal flats in Hainan Province are mainly distributed in the Beibu Bay area (including Danzhou Bay), accounting for 60.12%.The tidal flat of Taiwan Province will mainly be distributed in the northwest area, accounting for 97.12%.

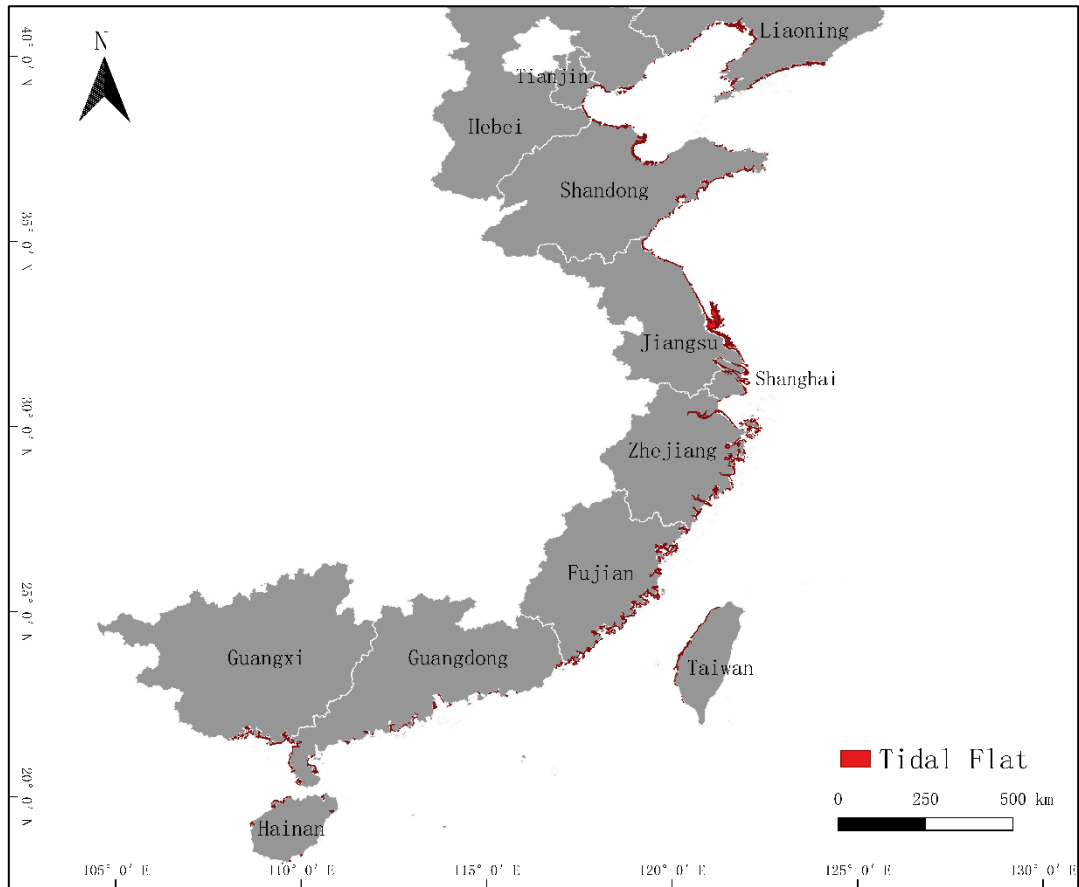


Figure 7. Distribution Map of Tidal Flats in China.

3.4. Tidal Flat Area Change in China, 2018-2023

The total area of China's tidal flat was 8300.34km² in 2018 and 8151.54km² in 2023, and the total area of China's tidal flat decreased by 148.80km² from 2018 to 2023. The specific information of the area of each provincial administrative unit in China in 2018 and 2023 is shown in Figure 8(a). As shown in Figure 8(b), among the 12 provincial administrative units, only Zhejiang Province, Shanghai and Fujian Province (ranked from large to small) have an increase in area from 2018 to 2023.

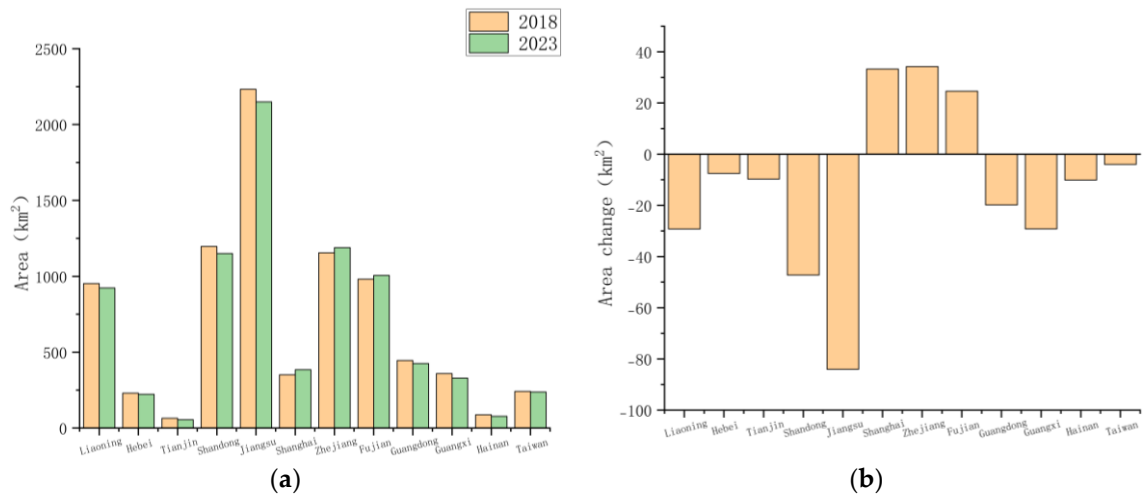


Figure 8. Tidal Flat Area and Changes in Coastal Provinces of China in 2018 and 2023:(a) Area in 2018 and 2023;(b) Change in Area from 2018 to 2023.

3.5. Coastline Information

In 2023, the total length of shoreline adjacent to tidal flats in China will be 10196.17km, with Fujian Province having the longest tidal flats (2220.45km), accounting for 21.78%, and Tianjin City having the shortest tidal flats (74.51km), accounting for 0.73%. Artificial shoreline and natural shoreline accounted for 67.06% and 32.94% respectively. The development degree of the tidal flat in China is 2.04, which indicates that most of the tidal flat has been developed and utilized. In terms of each provincial administrative unit, Tianjin Municipality has the highest degree of development (22.69), while Guangxi Province has the lowest degree of development (0.29) (Figure 9).

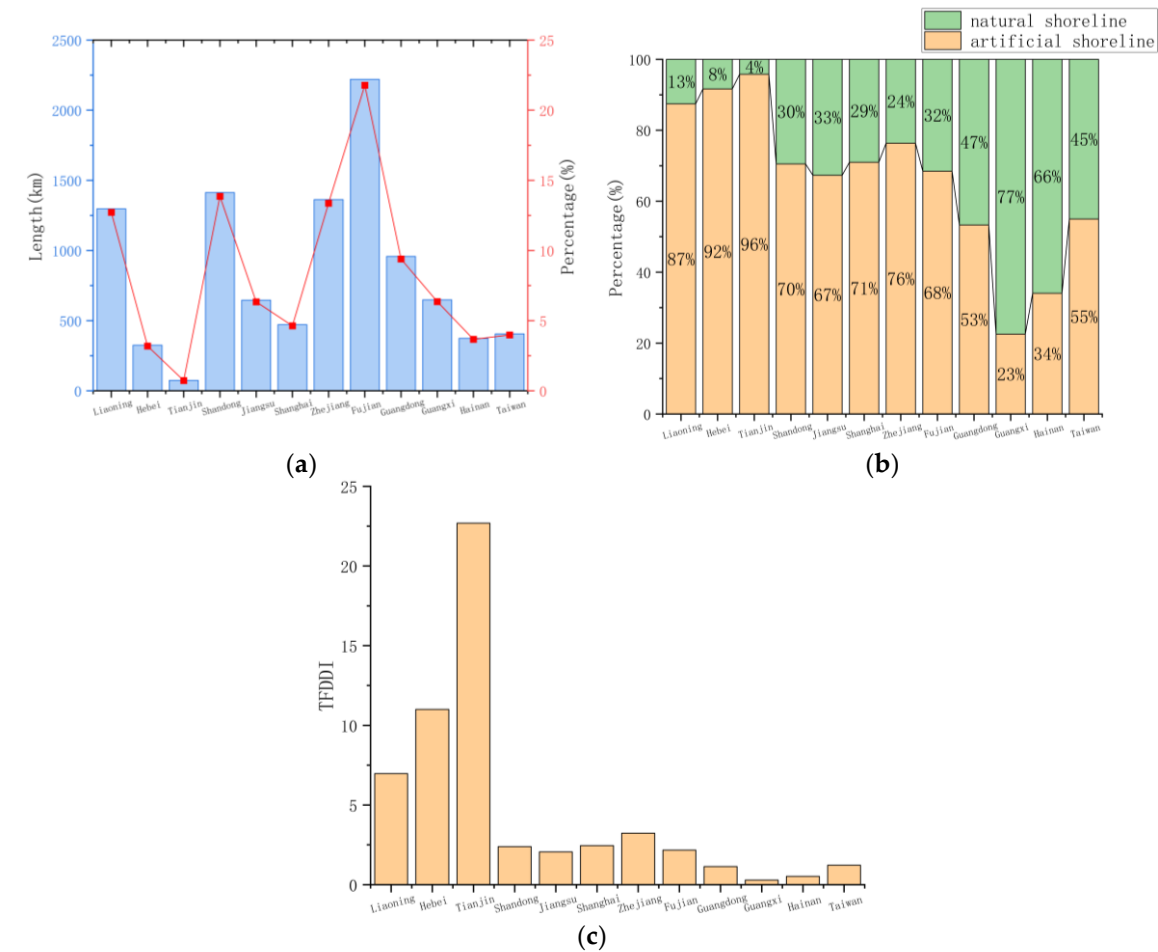


Figure 9. Shoreline Types and Development Intensity in China and Provinces:(a) Shoreline Length and Proportion;(b) Stacked Percentage Chart of Shoreline Classification;(c) Tidal Flat Development Intensity.

4. Discussion

In this paper, Sentinel-2 (MSI), Landsat8 (OLI) and Landsat9 (OLI-2) images were selected based on GEE platform, and a series of preprocessing including atmospheric correction, upsample and cloud removal were performed to construct a multi-source high-quality dense time series image collection. The spatial resolution of Sentinel-2 images was 10m. The revisit interval is 2-5 days, the high spatial resolution allows for more accurate identification of tidal flat boundaries, and the high temporal resolution provides a good opportunity to capture the lowest and highest tides. Compared with Sentinel-2 image data, the advantage of multi-source high-quality dense time series images is that the addition of Landsat 8 and Landsat 9 images increases the time resolution, making the lowest and highest water images obtained in this experiment more close to the real situation and more accurate and robust depiction of tides. Combined with previous research results [33], two appropriate spectral indices of mNDWI and NDVI were selected, and the MSIC-OA algorithm was combined to

realize rapid automatic classification and extraction of Chinese tidal flats. The detailed mapping of China's tidal flats in 2018 and 2023 has been realized, and the in-depth study of tidal flats has been carried out from the perspectives of resource stock, distribution characteristics, dynamic changes, utilization mode and development degree.

The traditional MSIC-OA algorithm extracts tidal flats in some areas including the tidal flats themselves and floating mud in seawater. In this study, an improvement of floating mud pixel elimination is proposed to solve this shortcoming, so as to make the extraction results more accurate.

The overall classification accuracy of Chinese tidal flat in 2023 is 95.19%, and the Kappa coefficient is 0.89. In 2018, it was 92.77% and 0.83. The results of qualitative and quantitative analysis show that the results of tidal flat extraction in this study are reliable. The imaging time range of Landsat 9 is 2021.10-2024.06, so this image was not used in the extraction of the tidal flat in 2018, which also makes the accuracy of the extraction results in 2018 slightly lower than that in 2023, which also proves the advantage of multi-source image set to some extent.

The total area of China's tidal flat in 2018 and 2023 is 8300.34km² and 8151.54km², respectively, and the area decreased by 148.80km² from 2018 to 2023. Among the 12 provincial administrative units, only Zhejiang Province, Shanghai and Fujian Province have an increase in area (ranking from large to small). Jiangsu Province, Shandong Province and Liaoning Province saw the largest decrease in area. In 2023, the tidal flat area of China's provinces in descending order is: Jiangsu, Zhejiang, Shandong, Fujian, Liaoning, Guangdong, Shanghai, Guangxi, Taiwan, Hebei, Hainan, Tianjin.

In 2023, 54.88% of the tidal flats in China will be distributed in estuaries and bays, 22.43% in estuaries and 32.45% in bays. Jiangsu Province has the largest tidal flat area, but only 5.25% is distributed in estuaries and bays. If Jiangsu Province is ignored, 72.64% of China's tidal flats are distributed in estuaries and bays, of which 29.74% are distributed in estuaries and 42.90% are distributed in bays. Most of China's tidal flats are located near river inlets and bays. The characteristics of easy sediment accumulation in estuaries and bays [34] are consistent with this conclusion.

In the analysis of shoreline, it is found that the total length of the shoreline adjacent to the tidal flat in China in 2023 is 10196.17km, the proportion of artificial shoreline is 67.06%, and the TFDDI is 2.04, indicating that most of the tidal flat has been significantly affected and changed by human activities. In particular, Tianjin has the highest development degree of tidal flat at 22.69, which may be closely related to the process of urbanization and industrialization, reminding us that the relationship between ecological protection and economic development should be balanced in the utilization of tidal flat resources.

In future studies, if more sources or higher resolution image data are provided for creating multi-source high-quality dense time series image collection to further improve its temporal and spatial resolution, the accuracy of tidal flat extraction will be further improved.

5. Conclusion

Based on GEE platform, this paper constructs multi-source high-quality dense time series image collection, and combines the improved MSIC-OA algorithm to achieve the extraction and analysis of tidal flats in China in 2018 and 2023. The conclusions are as follows:

- The overall classification accuracy of the tidal flat extraction results in China in 2018 was 92.77%, with an area of 8300.34km²; In 2023, the overall classification accuracy is 95.19%, and the area is 8151.54km². A decrease of 148.80km² from 2018 to 2023.
- The three provinces with the largest tidal flat area in 2023 are: Jiangsu, Zhejiang and Shandong
- In 2023, 54.88% of China's tides will be distributed in the river and bay areas, and if Jiangsu Province is not considered, the proportion rises to 72.64%. Most of China's tidal flats are located near river inlets and bays.
- In 2023, the total length of China's coastline adjacent to the tidal flat will be 10196.17km. The development degree of the tidal flat is 2.04, and most of the tidal flat has been developed and utilized.

References

1. Murray N J, Phinn S R, Clemens R S, et al. Continental scale mapping of tidal flats across East Asia using the Landsat archive[J]. *Remote Sensing*, 2012, 4(11): 3417-3426.
2. Wang X, Xiao X, Zou Z, et al. Tracking annual changes of coastal tidal flats in China during 1986–2016 through analyses of Landsat images with Google Earth Engine[J]. *Remote Sensing of Environment*, 2020, 238: 110987.
3. Wang X, Xiao X, Zou Z, et al. Mapping coastal wetlands of China using time series Landsat images in 2018 and Google Earth Engine[J]. *ISPRS Journal of Photogrammetry and Remote Sensing*, 2020, 163: 312-326.
4. Barbier E B, Koch E W, Silliman B R, et al. Coastal ecosystem-based management with nonlinear ecological functions and values[J]. *science*, 2008, 319(5861): 321-323.
5. Dhanjal-Adams K L, Hanson J O, Murray N J, et al. The distribution and protection of intertidal habitats in Australia[J]. *Emu-Austral Ornithology*, 2016, 116(2): 208-214.
6. Ghosh S, Mishra D R, Gitelson A A. Long-term monitoring of biophysical characteristics of tidal wetlands in the northern Gulf of Mexico—A methodological approach using MODIS[J]. *Remote Sensing of Environment*, 2016, 173: 39-58.
7. Tiner R W. Tidal wetlands primer: an introduction to their ecology, natural history, status, and conservation[M]. University of Massachusetts Press, 2013.
8. Murray N J, Ma Z, Fuller R A. Tidal flats of the Yellow Sea : A review of ecosystem status and anthropogenic threats[J]. *Austral Ecology*, 2015, 40(4): 472-481.
9. Deegan L A, Johnson D S, Warren R S, et al. Coastal eutrophication as a driver of salt marsh loss[J]. *Nature*, 2012, 490(7420): 388-392.
10. Gardner R C, Finlayson C. Global wetland outlook: state of the world's wetlands and their services to people[C]//Ramsar convention secretariat. 2018: 2020-5.
11. Cf O. Transforming our world: the 2030 Agenda for Sustainable Development[J]. United Nations: New York, NY, USA, 2015.
12. Arkema K K, Guannel G, Verutes G, et al. Coastal habitats shield people and property from sea-level rise and storms[J]. *Nature climate change*, 2013, 3(10): 913-918.
13. Zhu Z, Vuik V, Visser P J, et al. Historic storms and the hidden value of coastal wetlands for nature-based flood defence[J]. *Nature Sustainability*, 2020, 3(10): 853-862.
14. Hou X Y, Wu T, Hou W, et al. Characteristics of coastline changes in mainland China since the early 1940s[J]. *Science China Earth Sciences*, 2016, 59: 1791-1802.
15. Mao D, Wang Z, Wu J, et al. China's wetlands loss to urban expansion[J]. *Land degradation & development*, 2018, 29(8): 2644-2657.
16. Xu N, Gong P. Significant coastline changes in China during 1991–2015 tracked by Landsat data[J]. *Sci. Bull*, 2018, 63(14): 883-886.
17. Ma Z, Melville D S, Liu J, et al. Rethinking China's new great wall[J]. *Science*, 2014, 346(6212): 912-914.
18. Guo Q, Pu R, Tapley K, et al. Impacts of coastal development strategies on long-term coastline changes: a comparison between Tampa Bay, USA and Xiangshan Harbor, China[J]. *Papers in Applied Geography*, 2019, 5(1-2): 126-139.
19. NDRC, Ministry of Natural Resources. The national major project overall planning of important ecosystem protection and restoration (2021-2035) [EB/OL]. (2020-06-12) [2021-07-01] HTTP: / / http://www.gov.cn/zhengce/zhengceku/2020-06/12/content_5518982.htm
20. Sun Z, Sun W, Tong C, et al. China's coastal wetlands: conservation history, implementation efforts, existing issues and strategies for future improvement[J]. *Environment International*, 2015, 79: 25-41.
21. Xu W, Xiao Y, Zhang J, et al. Reply to Yang et al.: Coastal wetlands are not well represented by protected areas for endangered birds[J]. *Proceedings of the National Academy of Sciences*, 2017, 114(28): E5493-E5493.
22. Yang H, Ma M, Thompson J R, et al. Protect coastal wetlands in China to save endangered migratory birds[J]. *Proceedings of the National Academy of Sciences*, 2017, 114(28): E5491-E5492.
23. Meng W, Hu B, He M, et al. Temporal-spatial variations and driving factors analysis of coastal reclamation in China[J]. *Estuarine, Coastal and Shelf Science*, 2017, 191: 39-49.
24. Zhao C, Qin C Z, Teng J. Mapping large-area tidal flats without the dependence on tidal elevations: A case study of Southern China[J]. *ISPRS journal of photogrammetry and remote sensing*, 2020, 159: 256-270.
25. Tian B, Wu W, Yang Z, et al. Drivers, trends, and potential impacts of long-term coastal reclamation in China from 1985 to 2010[J]. *Estuarine, Coastal and Shelf Science*, 2016, 170: 83-90.
26. Mueller-Navarra K, Milker Y, Bunzel D, et al. Evolution of a salt marsh in the southeastern North Sea region—anthropogenic and natural forcing[J]. *Estuarine, Coastal and Shelf Science*, 2019, 218: 268-277.
27. Jiang W, Lv J, Wang C, et al. Marsh wetland degradation risk assessment and change analysis: A case study in the Zoige Plateau, China[J]. *Ecological Indicators*, 2017, 82: 316-326.

28. Cozzoli F, Smolders S, Eelkema M, et al. A modeling approach to assess coastal management effects on benthic habitat quality: A case study on coastal defense and navigability[J]. *Estuarine, Coastal and Shelf Science*, 2017, 184: 67-82.
29. Xu Y, Cai Y, Sun T, et al. Coupled hydrodynamic and ecological simulation for prognosticating land reclamation impacts in river estuaries[J]. *Estuarine, Coastal and Shelf Science*, 2018, 202: 290-301.
30. Wang Y P, Gao S, Jia J, et al. Sediment transport over an accretional intertidal flat with influences of reclamation, Jiangsu coast, China[J]. *Marine Geology*, 2012, 291: 147-161.
31. Garcia-Oliva M, Hooper T, Djordjević S, et al. Exploring the implications of tidal farms deployment for wetland-birds habitats in a highly protected estuary[J]. *Marine Policy*, 2017, 81: 359-367.
32. de Vriend H J. Ecosystem-based coastal defence in the face of global change[J]. *Nature: International Weekly Journal of Science*, 2013 (7478).
33. Jia M, Wang Z, Mao D, et al. Rapid, robust, and automated mapping of tidal flats in China using time series Sentinel-2 images and Google Earth Engine[J]. *Remote Sensing of Environment*, 2021, 255: 112285.
34. Wang Y, Zhu D K: Tidal flats in China, *Oceanology of China Seas*: Springer, 1994: 445-456.

Disclaimer/Publisher's Note: The statements, opinions and data contained in all publications are solely those of the individual author(s) and contributor(s) and not of MDPI and/or the editor(s). MDPI and/or the editor(s) disclaim responsibility for any injury to people or property resulting from any ideas, methods, instructions or products referred to in the content.